Jin,X, Zhang,J, Gao,W, Li,J and Wang,X 2014, Cocoon of the silkworm Antheraea pernyi as an example of a thermally insulating biological interface., Biointerphases, vol. 9, no. 3, pp. 031013-1-031013-11.

Cocoon of the silkworm *Antheraea pernyi* as an example of a thermally insulating biological interface

Xing Jin, Jin Zhang,[a)] Weimin Gao, and Jingliang Li
Australian Future Fibres Research and Innovation Centre, Institute for Frontier Materials, Deakin University, VIC 3216, Australia

Xungai Wang[a)]
Australian Future Fibres Research and Innovation Centre, Institute for Frontier Materials, Deakin University, VIC 3216, Australia and School of Textile Science and Engineering, Wuhan Textile University, Wuhan 430073, China

(Received 12 June 2014; accepted 11 July 2014; published 24 July 2014)

Biological materials are hierarchically organized complex composites, which embrace multiple practical functionalities. As an example, the wild silkworm cocoon provides multiple protective functions against environmental and physical hazards, promoting the survival chance of moth pupae that resides inside. In the present investigation, the microstructure and thermal property of the Chinese tussah silkworm (*Antheraea pernyi*) cocoon in both warm and cold environments under windy conditions have been studied by experimental and numerical methods. A new computational fluid dynamics model has been developed according to the original fibrous structure of the *Antheraea pernyi* cocoon to simulate the unique heat transfer process through the cocoon wall. The structure of the *Antheraea pernyi* cocoon wall can promote the disorderness of the interior air, which increases the wind resistance by stopping most of the air flowing into the cocoon. The *Antheraea pernyi* cocoon is wind-proof due to the mineral crystals deposited on the outer layer surface and its hierarchical structure with low porosity and high tortuosity. The research findings have important implications to enhancing the thermal function of biomimetic protective textiles and clothing. © *2014 American Vacuum Society*. [http://dx.doi.org/10.1116/1.4890982]

I. INTRODUCTION

A silkworm cocoon is made of silk fibers that are spun around the silkworm pupa when it is undergoing transformation. Thin and lightweight wild cocoons can protect silkworms from harsh weather conditions (−40 to 50 °C), physical attacks and other environmental adversaries, while supporting their metabolic activity. Yet outside the cocoon, wild silkworms would not survive in very cold weather. A perennial problem for the development of protective clothing is the difficulty in realizing both protection and comfort for the wearer. Clothing with good protection against extreme weather conditions is usually heavy and bulky with poor breathability, hence uncomfortable to wear. Learning from wild silkworm cocoons could be an effective way of designing novel breathable materials for enhanced thermal protection and comfort.

More than 5000 years ago, the practice of breeding silkworms for the production of raw silk commenced in China.[1] It then spread to Korea and Japan, and later to India and Western countries. Nowadays, *Bombyx mori* (*B. mori*), which was domesticated from *Bombyx mandarina*,[2,3] is the main silk source in the world. In addition to *B. mori,* several types of silkworms have also been used as silk sources, including the semidomestic *Samia cynthia*,[4] the wild *Antheraea pernyi (A. pernyi)*[5] and the wild *Antheraea mylitta*.[6] Depending on silk species, silkworm silk fibers can have tensile strength of about 500 MPa and Young's modulus of about 10 GPa, with breaking strain of 20%–40%,[7] which makes silk one of the toughest fibers.[8] In addition, silkworm silk fibers have excellent thermal insulation properties. They have low thermal conductivity (0.15–1 W/(m·k) and low moisture regain under standard conditions (about 12%–14%, at the temperature of 273.15 K and absolute pressure of 100 kPa).[9,10]

A silkworm cocoon is a light porous multilayer structure, constructed from continuous twin silk filaments (fibroin) bonded by silk gum (sericin). From the composite materials point of view, a silkworm cocoon can be considered as a porous matrix of sericin reinforced by randomly oriented continuous silk fibroin.[11,12] Pores with different sizes are located between the silk filaments and they can be either interconnected or disconnected.[13] As the silk spinning continues toward the center, the silk filaments become finer, which can be seen from the comparison between the outer layer [Figs. 1(b) and 1(e)] and inner layer [Figs. 1(c) and 1(f)] of the cocoons. It has also been found that the silk fibers become stronger toward the inner layers of the cocoon, as a result of the increased crystallinity and molecular orientation of silk polymer.[14,15] The fiber width is generally larger for the cocoon outer layers than the inner layers and the fibers in the inner layers are arranged more compactly than those in the outer layers. In contrast to the domestic *B. mori* cocoon, the structure of the Chinese tussah silkworm *A. pernyi* cocoon is more compact; on the outer surface of the *A. pernyi* cocoon wall, cubic mineral crystals are present on

a)Authors to whom correspondence should be addressed; electronic addresses: jin.zhang@deakin.edu.au; xungai.wang@deakin.edu.au

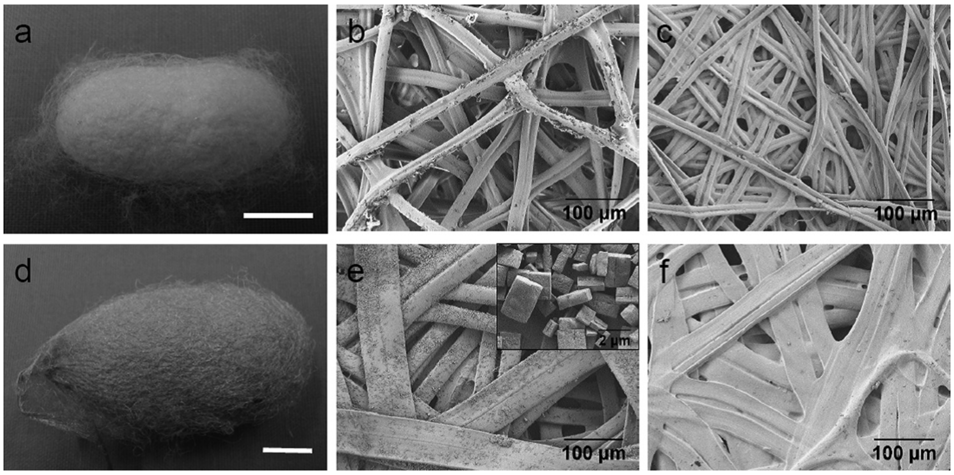

FIG. 1. Silk cocoon morphology. (a) The *B. mori* cocoon; (b) and (c) show the outer and inner layer surfaces of the *B. mori* cocoon, respectively; (d) the *A. pernyi* cocoon; (e) the outer layer surface of the *A. pernyi* cocoon (inset shows the mineral crystals on the surface); and (f) the inner layer surface of the *A. pernyi* cocoon. The white scale bars are 10 mm.

the surface of silk fibers and in the pores [the inset of Fig. 1(e)]. These crystals have been identified as calcium oxalates, which are the excrement left by the silkworm during spinning.[16] The crystals have been suggested to contribute to the water resistance of the cocoon,[17,18] and the preferential gating of CO_2 from cocoon inside to outside[17] In contrast to the *A. pernyi* cocoon, there are no crystals on the outer surface of the *B. mori* cocoon.

As a multilayered and graded structure, the microstructure and mechanical properties of silk cocoons have been previously studied for enhancing the survival chance of silkworms against physical attack and environmental damage.[19–22] However, very limited research has been conducted on the thermal protective properties and functions of silkworm cocoons. Zhang *et al.* investigated the thermal insulation properties of both domestic and wild silkworm cocoons under warm conditions (from ambient temperature to 50 °C).[23] They have found that the silkworm cocoons are able to provide significant buffer against temperature changes outside the cocoon structure and the wild cocoons show stronger thermal buffer function over the domestic cocoon types. Avazov recently reported a mathematical model to calculate temperatures at different positions in the thickness direction of domestic cocoon shell on exposure to IR radiation.[24] Silk cocoons are exposed to heat or radiations prior to reeling of silk filament for textile processing. It is important not to have adverse impacts on silk fiber properties during such treatments. From such a perspective, Avazov's model considered the heat absorption of cocoon and pupae, the thermal conductivity of cocoon shell, the temperature gradient between cocoon walls and the inner and outer environment to calculate the cocoon shell temperature.

The principal function of clothing is to maintain the human body in an acceptable thermodynamic state under different environmental conditions and during various body activities.[25] Thermal comfort is the most essential factor in maintaining the health and satisfaction of the wearer. At present, high thermal protection has been achieved by using ceramic fibers or synthetic fibers coated or filled with inorganic fillers, such as zirconium magnesium oxide or iron oxide. Such materials are heavy and inflexible and have poor breathability, hence uncomfortable to wear. Understanding how wild silk cocoons maintain thermal comfort for the pupa residing inside provides a solid foundation for designing future flexible thermal functional materials. In this work, both experimental and numerical methods were used to study the thermal insulation properties and the heat transfer process of the wild *A. pernyi* cocoon under windy conditions. Important factors including temperature (45 and 4 °C isothermal settings representing the warm and the cold conditions), cocoon type and mineral crystals were investigated. The results may have significant implications to the design and development of future protective textile materials.

II. MATERIALS AND METHODS

A. Materials

Both the domestic *B. mori* and the wild *A. pernyi* cocoons were used in this investigation. The *B. mori* cocoons were cultivated in the Physics Laboratory of National University of Singapore and the *A. pernyi* cocoons were collected from Northeast China. Some of the *A. pernyi* cocoons were demineralized (i.e., the mineral crystals were removed from the outer surface) using a ultrasonication method as illustrated in Ref. 26. The length and width of the *Bombyx mori* cocoon used were about 35 and 19 mm, respectively, and the length and width of the *A. pernyi* cocoons used in the experiment were about 50 and 26 mm, respectively.

B. Scanning electron microscopy

The cocoon wall surfaces and layers and its cross sections were observed by a Supra 55 VP scanning electron microscope (SEM) after the samples were sputter coated with gold. The cross sections were obtained by embedding the cocoon wall into an epoxy matrix and then ground wet through

80, 240, 600, 1200, and 4000 grit silicon carbide abrasive paper.

C. Temperature monitoring under windy conditions

To simulate natural windy conditions, an artificial air flow field was created using an electric fan (DC 12 V, 0.2 A) and a connected duct (a plastic tube with the same diameter as the fan). The experimental set-up is shown in Fig. 2. The cocoons were translocated from ambient environment to the middle of the duct through a hole at the bottom, while this ventilation system was situated in an oven (Binder) with isothermal setting of 45 °C or in a fridge (Thermo scientific) with isothermal setting of 4 °C. The electric fan was driven by a power source (Powertech™ MP 3081 DC power supply, 0–30 V, 0–3 A), and the wind velocity was adjusted by changing the voltage output. Two needle-type temperature probes (from ICT SFM, a sap flow meter produced by ICT international Pty. Ltd.)[23] were used to measure the temperature both inside and outside the cocoons. Each temperature probe is 1.3 mm in diameter and 35 mm in length, with two sensors located 15 mm apart (one of the sensors is 7 mm distant from the needle tip). The temperature probe outside was located about 10 mm away from the cocoon surface. The wind velocity was measured by a hot-wire anemometer (TES-1341). For every type of cocoon, three samples were tested for each measurement and the standard deviations were indicated in the graphs as error bars. In this artificial flow field, the wind velocity was set at 0.7 m/s to simulate a natural breeze. The duration of the experiments in the oven and fridge were 1200 and 600 s, respectively.

D. Numerical model set-up and development

The commercial computational fluid dynamics (CFD) code CFX 14.5 from ANSYS Inc.[27] was used for simulating the heat transfer process through the wild *A. pernyi* cocoon wall in the flow field. The model aims at understanding how the microstructure of cocoon wall affects the heat transfer process through it. Due to the complexity of the fibrous microstructure of the cocoon wall, the use of a two-dimensional cross section of a cylinder would consume great amount of simulation time in mesh and calculation. A two-dimensional model based on a rectangular piece of the *A. pernyi* cocoon wall using its geometrical configuration [Fig. 3(a)] was therefore built to simulate the heat transfer process through the cocoon wall, with reduced requirement of simulation time and operational capability. The cross section of the cocoon wall is composed of three main sections, i.e., the outer section, the middle section and the inner section. The cross-sectional dimensions of silk fibers in each section were defined according to the average values of measured data from the SEM image [Fig. 3(b)].

In the model, the silk fibers in each section have identical geometrical configuration and are arranged in a regular manner. The cross section of silk fibers was simulated with an ellipse shape. The parameters to define the cocoon wall structure include the length and the width of the silk fiber cross section, the gap between two adjacent fibers along the length direction (x-axis) and along the width direction (y-axis), the location offset values between the adjacent rows and the total number of rows in each section. Table I gives the geometrical parameter inputs into the model. The porosity of the 2D cocoon model is 0.66, which is in accordance with the tested data 0.67 ± 0.030.[28] The thickness of the 2D cocoon model (the distance along the y-axis direction) is 450 μm, which is similar to the data 430 ± 70 μm recorded from the *A. pernyi* cocoon in Ref. 18. The length of the cocoon model (the distance along the x-axis direction) is 600 μm. To model the surroundings inside the cocoon, a space with thickness of 100 μm was extended from the inner surface of the cocoon. To model the surroundings outside the cocoon, a space with the thickness of 310 μm was extended from the outer surface of the cocoon. To connect the mesh in the cocoon wall and the main flow domain, a transition

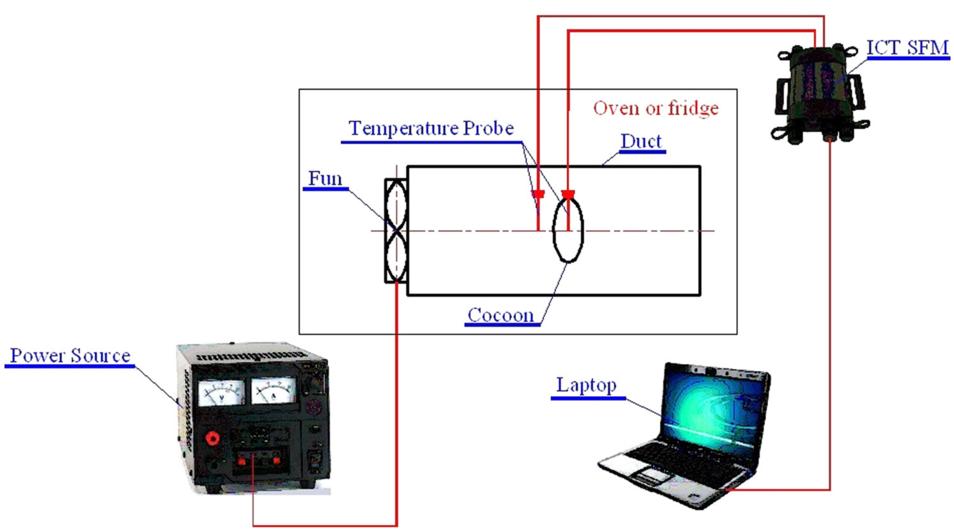

FIG. 2. Experimental set-up for thermal measurement of silkworm cocoons.

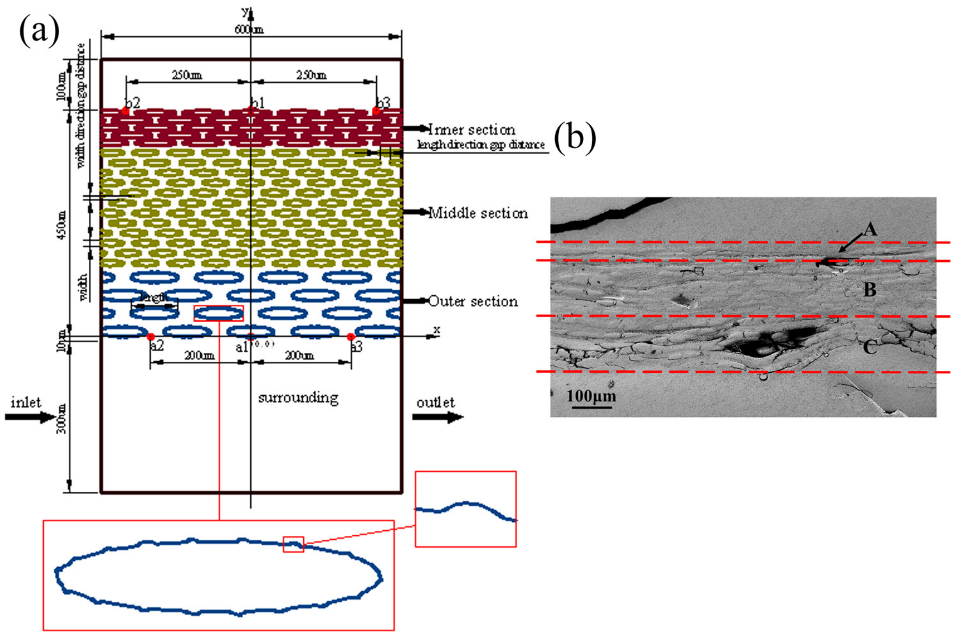

FIG. 3. Cocoon wall model constructed according to the original *A. pernyi* cocoon wall structure. (a) Geometrical configuration of the model (the cross section of the silk fibers is shown elliptical and the vacant region is the channel for air flow); (b) SEM image of the cocoon wall structure (A—the inner section; B—the middle section; C—the outer section).

domain with a thickness of 10 μm was built between these two regions. The mesh of the model is shown in Fig. 4. The model does not distinguish the silk fibroin from sericin and the silk fibers were treated as a whole in the model.

The thermal conductivity of silk is more than 0.54 W/(m K),[29] while the thermal conductivity of crystals is about 0.22 W/(m K).[23] It is apparent that the crystals have higher thermal resistance over the silk. Since the crystals are located on the surface of cocoon outer layer, the roughness of the silk fibers is increased, which therefore increases the flow resistance along the silk fiber.[30] In order to study the effects of crystals on the heat transfer process, embossment was created on the silk fiber surface in the outer layers of *A. pernyi* cocoon. For simulation, the following assumptions were introduced:

(1) The *A. pernyi* cocoon wall is homogeneous in terms of fiber arrangement and material properties;
(2) The air is ideal gas and the main direction of flow is along the outer surface of the cocoon;
(3) No shrinking, expansion or movement of the cocoon structure occurs during heat transfer;
(4) The air channels are much larger than the mean free path of the fluid molecules thus the continuum hypothesis holds.

TABLE I. Geometrical parameters used for the 2D model of the *A. pernyi* cocoon wall.

	Width (μm)	Length (μm)	Gap distance in width direction (μm)	Gap distance in length direction (μm)	Total number of rows
Inner layer region	10	80	5	15	5
Middle layer region	11	40	9	20	12
Outer layer region	20	92	16	36	4

E. Mathematical formulation

An integral expression for the balance of energy has been given by the first law of thermodynamics. Based on the conservation of heat energy, the heat transfer equation (see the nomenclature) can be written as follows:[31,32]

$$\mathrm{c_v}\frac{\partial \mathrm{T}}{\partial \mathrm{t}} = \underbrace{-\varepsilon \mathrm{u c_{va}} \nabla \mathrm{T}}_{\text{Convection}} + \underbrace{\lambda \nabla^2 \mathrm{T}}_{\text{Conduction}} + \underbrace{\nabla \mathrm{F}}_{\text{Radiation}} + \underbrace{\kappa \Gamma}_{\text{Latent heat}} . \tag{1}$$

For the heat transport through the fibrous cocoon batting, mechanisms such as thermal conduction, convection, radiation, and release and absorption of latent heat by phase changes can affect the process simultaneously.[33] Under the current experimental conditions, thermal conduction and thermal convection play a major role in the heat transfer process, whereas radiation and the latent heat can be neglected. The heat transfer equation [Eq. (1)] can therefore be simplified as

$$\mathrm{c_v}\frac{\partial \mathrm{T}}{\partial \mathrm{t}} = \underbrace{-\varepsilon \mathrm{u c_{va}} \nabla \mathrm{T}}_{\text{Convection}} + \underbrace{\lambda \nabla^2 \mathrm{T}}_{\text{Conduction}} , \tag{2}$$

where u is the flow velocity of air in the cocoon wall, which is calculated by Navier–Stokes equations[32]

$$\mathrm{H}(u - \bar{u}) + (1 - \mathrm{H})(-\nabla \mathrm{p} + \nabla \cdot \bar{T} + \rho \mathrm{g} - \rho \mathrm{a}) = 0. \tag{3}$$

For the numerical calculation using ANSYS CFX, thermal conduction and convection were considered as the main contributing factors to the heat transfer process, which is described in Eq. (2). The initial pressure of the air in the model was set as zero and the initial temperature in the

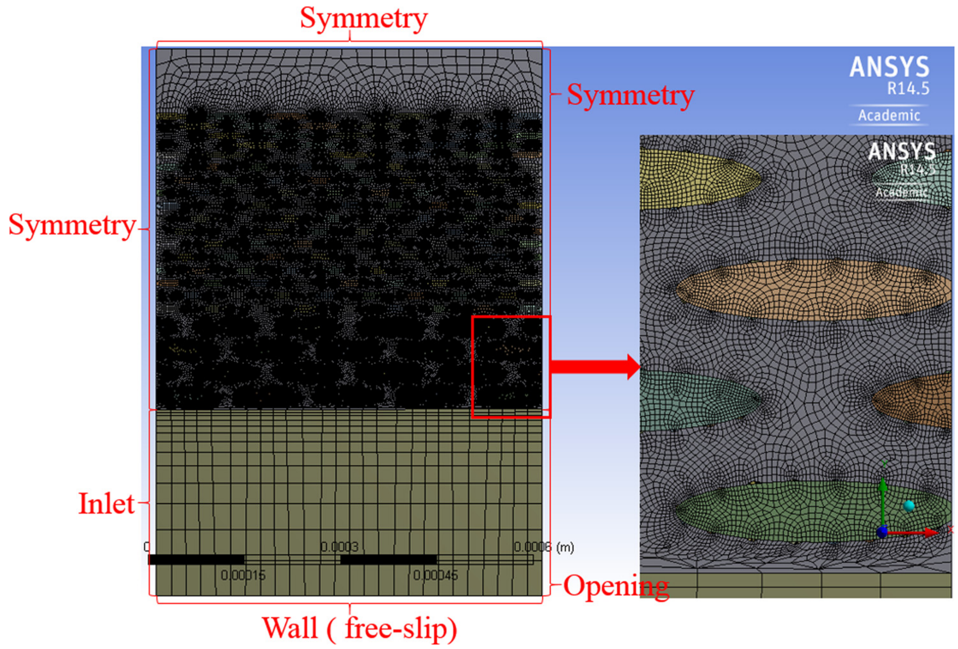

FIG. 4. Mesh and boundary conditions of the model.

model was taken from the temperature values in the beginning of each experiment. The boundary conditions are shown in Fig. 4. The surrounding temperatures vary with time and can be described by $T_s(t)$. The inlet temperature and wind velocity were taken from the experimental data and the relative pressure of outlet was zero. The opposite side of the cocoon wall in the surrounding was set as "free-slip" wall to neglect the viscous effect; the other faces except for interfaces were set as "symmetry" to indicate the symmetrical characteristic of the 2D model.

III. RESULTS

A. Comparison of thermal insulation between the domestic *B. mori* and the wild *A. pernyi* cocoon under windy conditions

Both the domestic *B. mori* cocoon and the wild *A. pernyi* cocoon were tested in the artificial windy flow field that was installed in the oven or fridge. Figure 5 shows the temperature profiles of locations inside the *B. mori* cocoon and the *A. pernyi* cocoon. The temperature in the oven was set at 45 °C and the temperature in the fridge was set at 4 °C; the wind velocity was set at 0.7 and 1.3 m/s, respectively.

The temperature difference (ΔT) between the *A. pernyi* cocoon and the *B. mori* cocoon was calculated by

$$\Delta T = T_{A.\,pernyi\text{–in}} - T_{B.\,mori\text{–in}}, \tag{4}$$

where $T_{A.\,pernyi\text{-in}}$ is the inside temperature of the *A. pernyi* cocoon and the $T_{B.\,mori\text{-in}}$ is the inside temperature of the *B. mori* cocoon. In the beginning of the heat transfer process, when the temperature difference between surrounding and inside temperature was high, the temperature increasing (decreasing) rate inside the *B. mori* cocoon was higher than that inside the *A. pernyi* cocoon. The highest inside temperature changing rates for the *A. pernyi* cocoon under these four conditions (shown in Fig. 5) were 3.5, 4.1, 5.5, and 4.9 °C/min, respectively; while the changing rates for the *B. mori* cocoon were 4.8, 5.1, 6.2, and 6.5 °C/min, respectively. As a result, the *A. pernyi* cocoon showed relatively slower changing rates and therefore more significant thermal buffer than the domestic *B. mori* cocoon. As the cocoon inside temperature approached the surrounding temperature, the temperature difference between two cocoons decreased after reaching a maximum value.

Wind is a critical factor that can alter thermal insulation. In the natural environment where wild silkworms live, wind can remove the relatively motionless insulating air on the outer surface and in the interior of the cocoon wall therefore impair its intrinsic insulation function. The cocoons that have excellent insulation properties relying on still air trapped in the cocoon walls could lose the function easily under windy conditions. However, the wild silkworm cocoon with crystals on the outer surfaces could lessen wind penetration and therefore effectively maintain thermal insulation under windy conditions. To further study the structural influence of the wild *A. pernyi* cocoon including the effect of mineral crystals in the outer layers, a computational model was built to simulate the *A. pernyi* cocoon wall, which will help clarify its thermal insulation mechanism under windy conditions.

B. Comparison of modeling data and experimental results for the *A. pernyi* cocoon

Figure 6 shows the predicted cocoon interior temperature from the models in comparison with experimental data (temperature both inside the cocoon and outside the original cocoon). Initially, the temperature difference between the

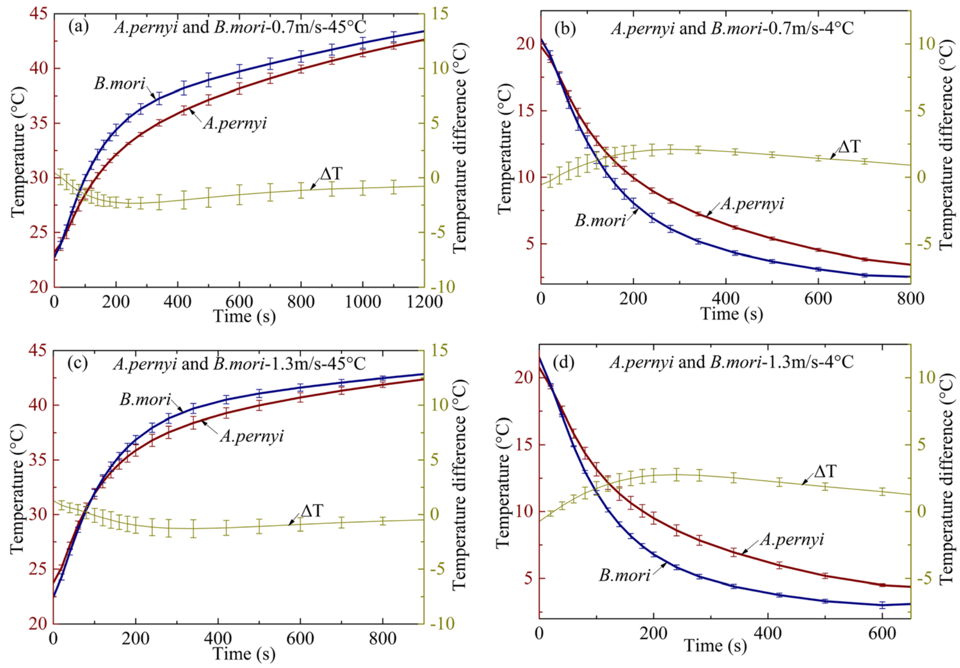

FIG. 5. Temperature profiles for locations both inside the *A. pernyi* cocoon and the *B. mori* cocoon under windy conditions. (a) and (c) in the oven with isothermal setting of 45 °C; (b) and (d) in the fridge with isothermal setting of 4 °C. The wind velocity is 0.7 m/s for (a) and (b) and is 1.3 m/s for (c) and (d).

surrounding and the inner cocoon was higher, so the heat flow rate was larger; the temperature inside the cocoon then changed quickly toward the surrounding temperature, which was driven by the higher temperature gradient of thermal conduction. In time, the temperature difference decreased so the changing rate of the temperature inside the cocoon became slower due to weakened thermal conduction. It can be seen from Fig. 6 that the results calculated from the present model agree reasonably well with the experimental data for the original *A. pernyi* cocoon.

C. Effect of crystals on the heat transfer through the *A. pernyi* cocoon wall

To study the function of crystals on the outer layers of the *A. pernyi* cocoon, the embossments on the silk fiber surface of cocoon outer layers, which represent the deposited crystals, were removed in the modified model. Under the same conditions as those used for the original cocoon, the numerical results of the temperature inside the demineralized cocoon were obtained and also shown in Fig. 5. It can be clearly seen that the inner temperature profile of demineralized cocoon is much closer to the outer temperature profile, which indicates that the thermal resistance of the cocoon wall decreased after demineralization treatment. However, the inner temperature profiles from the model without crystals do not fit the experimental data of demineralized cocoon as well as the case for the original cocoon, but are closer to the outer temperature profiles. The thermal conductivity of crystals is higher than the thermal conductivity of air,[23,34] which can increase the heat flux by thermal conduction. However, in the experimental conditions, the air is flowing

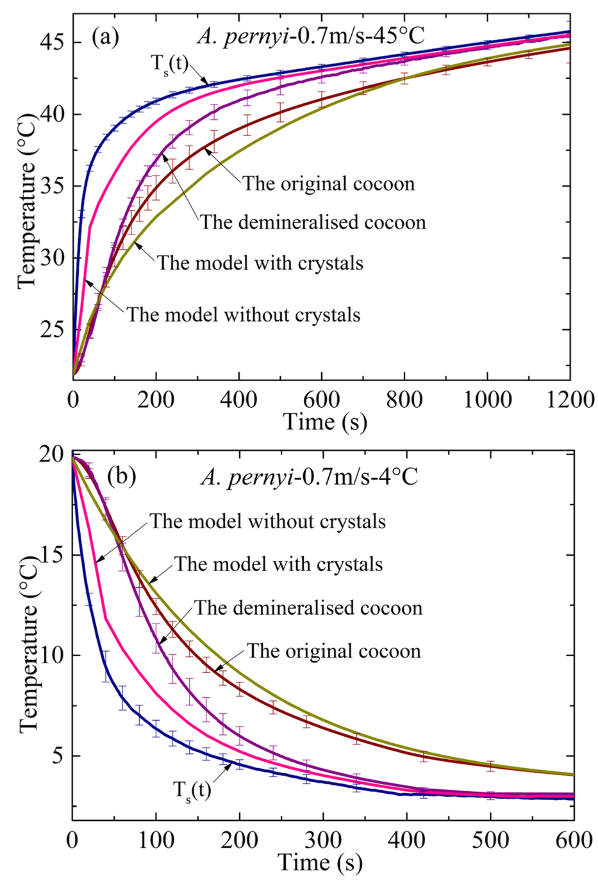

FIG. 6. Model predictions of the *A. pernyi* cocoon inner temperature changes under both warm (oven with isothermal setting of 45 °C) and cold (fridge with isothermal setting of 4 °C) conditions. (a) Under warm conditions and (b) under cold conditions.

inside the cocoon wall; therefore the heat transfer mechanism will differ from the static situation. Both thermal conduction and convection can take effect; in some cases, the thermal convection can play more important role than the thermal conduction.[35] As a result, it is necessary to study the functions of the crystals in affecting the microflow field within the cocoon wall.

Three positions on the inner and outer surfaces (indicated by a1, a2, and a3 for the outer surface and b1, b2, and b3 for the inner surface) were defined as shown in Fig. 3(a). a1 is in the center of the outer surface, and a2 and a3 are 200 μm away from the center; similarly, b1 is located in the center of the inner surface and b2 and b3 are 250 μm from the center. The static pressure of each position and the static pressure difference between the outer and inner cocoon surface were used to investigate the effect of mineral crystals on the microflow field. In the model, the air is supposed to flow along the surface of the cocoon, which is perpendicular to the direction of the air flowing through the cocoon wall. Therefore, the static pressure is one of the most important surrounding factors to influence the air flow process. For the cocoon with different structure under the same surrounding conditions, the air is easier to flow into the cocoon when the static pressure difference between outer and inner surfaces of the cocoon wall is higher. The static pressure profiles at these six positions from different models are shown in Fig. 7. It can be seen that the static pressure at the position b1, b2, and b3 are nearly the same under all conditions; the static pressure from the model with crystals fluctuates, while the static pressure from the model without crystals keeps steady. In the model without crystals, the static pressure on the outer surface of the cocoon decreases along the positive direction of x-axis, which is due to energy loss during flowing caused by the friction between the boundary of the cocoon wall and the fluid (air).[36] In contrast, for the model with crystals, the static pressure at point a3 (which is located in the silk fiber gap) is larger than the static pressure at point a1 (which is located on the surface of a fiber between two embossment).

The static pressure difference between the outer surface and inner surface of the cocoon wall can show the flow state of the air through the cocoon wall. The average value of static pressure at position a1, a2, and a3 was used as the static pressure value on the outer surface of the cocoon wall (P_{out}); The average value of static pressure at position b1, b2, and b3 was used as the static pressure value on the inner surface of the cocoon wall (P_{in}). The static pressure difference (ΔP) between the outer and inner surface of the cocoon wall was therefore calculated by

$$\Delta P_s = P_{out} - P_{in}. \tag{5}$$

Figure 8 shows the static pressure difference through the cocoon with crystals compared with the cocoon without crystals in the oven and fridge. It can be seen that the static pressure difference through the demineralized cocoon wall maintained a certain value at most of the time; however, the static pressure difference through the cocoon wall with crystals changed quickly. The static pressure difference through the demineralized cocoon wall is larger than the static

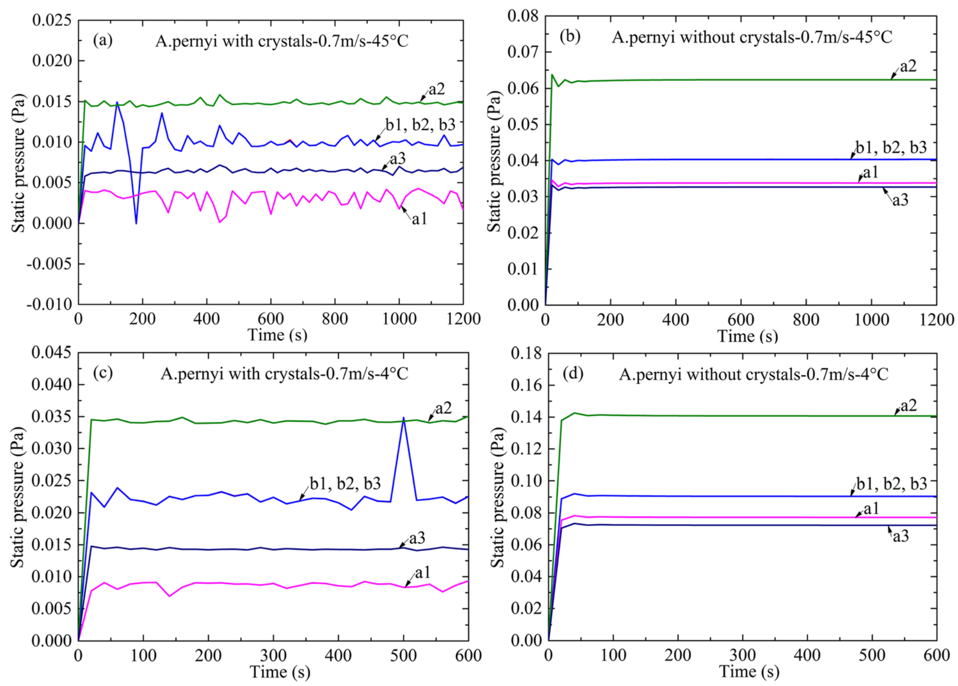

Fig. 7. Static pressure changes with time at specific locations [indicated in Fig. 3(a)] on the *A. pernyi* cocoon outer (a1, a2, and a3) and inner layer surfaces (b1, b2, and b3). (a) From the cocoon model with crystals tested under warm conditions (oven with isothermal setting of 45 °C); (b) from the model without crystals tested under warm conditions (oven with isothermal setting of 45 °C); (c) from the model with crystals tested under cold conditions (fridge with isothermal setting of 4 °C); and (d) from the model without crystals tested under cold conditions (fridge with isothermal setting of 4 °C).

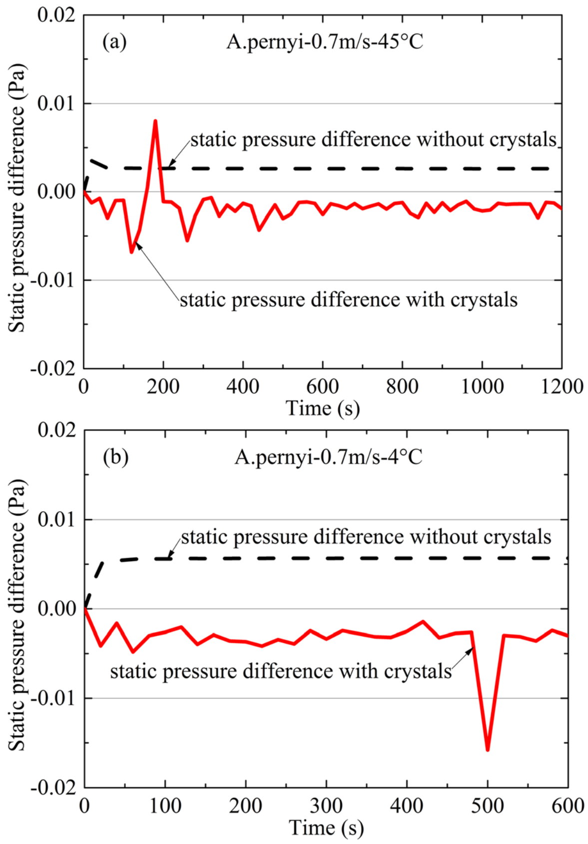

FIG. 8. Comparison of static pressure difference through the *A. pernyi* cocoon wall with and without crystals. (a) Under warm conditions (oven with isothermal setting of 45 °C); (b) under cold conditions (fridge with isothermal setting of 4 °C).

pressure difference through the cocoon wall with the crystals. Furthermore, the value of the static pressure difference through the cocoon wall with crystals remained negative during most of the time.

IV. DISCUSSION

A. Comparison between the domestic *B. mori* and the wild *A. pernyi* cocoon

A compact cocoon is formed when a silkworm, along with spinning, wraps the bave around its body through a gyrating motion of its head and cyclically bending and stretching of its body with different shapes in a programmed manner.[37,38] The cocoon structure can be considered as a porous matrix of sericin reinforced by randomly oriented continuous fibroin fibers.[39] The silkworm cocoons have a nonwoven composite structure with twin silk fibers coated with sericin. The cocoon outer surface and inner surface are remarkably different in terms of the silk fiber morphology, fiber width and the porous structure created by silk fibers. The fiber width is generally smaller for the cocoon inner surfaces than the outer surfaces.[23] The wild *A. pernyi* cocoon shows a more compact structure than the domesticated *B. mori* cocoon.[22] Cubic crystals can be found on the outer section of *A. pernyi* cocoon, loosely deposited on the surface of silk fibers and stacked in the pores. These crystals have been identified as calcium oxalates, which show unique functionality such as preferential gating of CO_2 transfer.[17,18]

Since the thickness of the *A. pernyi* cocoon wall and the *B. mori* cocoon wall are similar[23] and the density of the *A. pernyi* cocoon wall is higher than that of the *B. mori* cocoon wall, more air is stored in the *B. mori* cocoon wall. Under the experimental conditions, convection is unavoidable which increases the heat energy transfer. In the *A. pernyi* cocoon wall, the organizations of silk fibers is more compact and the gap among the fibers is much smaller and arranged with high tortuosity.[28] This kind of structure can weaken the convection and therefore reduce the heat transfer by convection, resulting in reduced heat flux through the cocoon wall.[40] It also explains why the temperature difference between the *A. pernyi* cocoon interior and *B. mori* cocoon interior was larger at the initial stage and decrease later. At the initial heat transfer stage, the temperature between the surrounding and the cocoon interior was larger so the natural convection was more drastic. The fiber structure of the *A. pernyi* cocoon wall assisted with reducing natural convection effectively. With the heat transfer time, the temperature difference between surrounding and interior became smaller, the insulation function of the *A. pernyi* cocoon wall was not as obvious and the temperature difference between the *A. pernyi* cocoon and *B. mori* cocoon interior decreased.

The silk fibers of the *B. mori* have near triangular cross section and the silk fibers of the *A. pernyi* have near rectangular cross section. In general, the silk fiber profiles vary along the out-of-plane direction of the cocoon wall. The silk organization of the *A. pernyi* cocoon is more compact and less porous than the *B. mori* cocoon, resulting in its higher thermal insulation properties, especially under windy conditions. In addition, the existence of the mineral crystals on the outer surface of the wild *A. pernyi* cocoon increases the wind resistance and therefore further enhances the thermal insulation property. The specific dimensional details of the *A. pernyi* cocoon wall are shown in Table I.

B. Comparison of modeling data and experimental results for the *A. pernyi* cocoon

The model with the consideration of crystals can express the heat transfer process through *A. pernyi* cocoon wall reasonably well with little deviation from the experimental curve. This may be caused by the following two reasons: first, the extra radiant heat transfer between the duct and the cocoon was neglected in the model. The radiant heat can be transferred from the object with high temperature to the object with low temperature,[41,42] and the heat flux by thermal radiation is affected by the temperature difference between these two objects.[43] At the initial heat transfer stage, the temperature difference between the duct and the cocoon was larger, which led to considerable heat flux by thermal radiation and made the model results deviate from the experimental data; second, the simplified model of the cocoon wall would affect the accuracy of the simulation results as well.

C. Structural influence of *A. pernyi* cocoon wall on heat transfer process

By comparison with the original *A. pernyi* cocoon, the inside temperature of the demineralized cocoon from experiments is much closer to the surrounding temperature (Fig. 5), which may indicate the enhancing effect of the mineral crystals on thermal resistance. In the comparison between demineralized cocoon and the model without crystals, the simulation results from the model without crystals are closer to the surrounding temperature than the experimental data from the demineralized cocoon, attributing to the demineralization treatment which not only removed the crystals but also may have varied the cocoon structure. The effect of crystals is shown from their influence on the microflow field in the cocoon wall. It indicates from numerical results that the static pressure distribution inside the cocoon is uniform with or without crystals; the existence of crystals makes the air close to the cocoon outer surface flow unsteadily, which can therefore increase the flow resistance. Although the height of the embossments is trivial, they show obvious influence on the static pressure, evidenced by the decreased static pressure at location a1 (Fig. 7).

The static pressure difference between the outer surface and the inner surface of the cocoon wall is shown in Fig. 8, which indicates that the crystals can make the air in the cocoon wall flow unsteadily and increase the wind resistance of the cocoon wall, i.e., the cocoon wall with crystals can prevent the air outside from flowing into the interior more effectively. In addition, the value of the static pressure difference through the cocoon wall with crystals is negative most of the time, i.e., the static pressure on the inner surface is larger than the static pressure on the outer surface of the cocoon wall. This characteristic will assist with stopping most of the surrounding air flowing into the cocoon. Figure 9 shows the air flow velocity streamlines from the model at 1200s in the oven. It indicates that most of the air flow occurred in the surrounding and only trivial amount of air can flow into the cocoon wall. In the small percentage of air flew into the cocoon wall, most of it flew through the cocoon wall and circulated back into the surrounding and the rest flew through the cocoon wall and reached the interior of the cocoon, which is in accordance with the results obtained from Fig. 8.

The above phenomena further indicate the wild *A. pernyi* cocoon wall has strong wind resistance by stopping the air flowing from the outside toward inside. When the air flows to the outer layer of the cocoon wall, due to the existence of mineral crystals, the flow direction of some air varies and mixes with other air. The change of the flow direction of the air further leads to the change of pressure in the outer layer of cocoon wall; under this circumstance, the vortex is generated. The vortex makes the air flow unsteadily and it is also easily generated in the middle and inner layers of the cocoon wall due to the smaller gap between silk fibers, even if there are no crystals on the surface of the these fibers. The generated vortex can make the air flow outwards and stop the air flowing in to the cocoon. The presence of the crystals disrupts the external flow and creates uneven pressures along the surface of the cocoon, which would give rise to transient lateral (as opposed radial) flow patterns. This also contributes to minimizing penetration of outside air into the inside of the cocoon. This characteristic of cocoon wall can reduce most of the heat flux by thermal convection and result in excellent thermal insulation property of the *A. pernyi* cocoon wall, especially under windy conditions. The silkmoth pupa can therefore be protected from the hazard caused by extreme weather conditions. Similarly, one-way carbon dioxide flow through the cocoon wall has been observed to

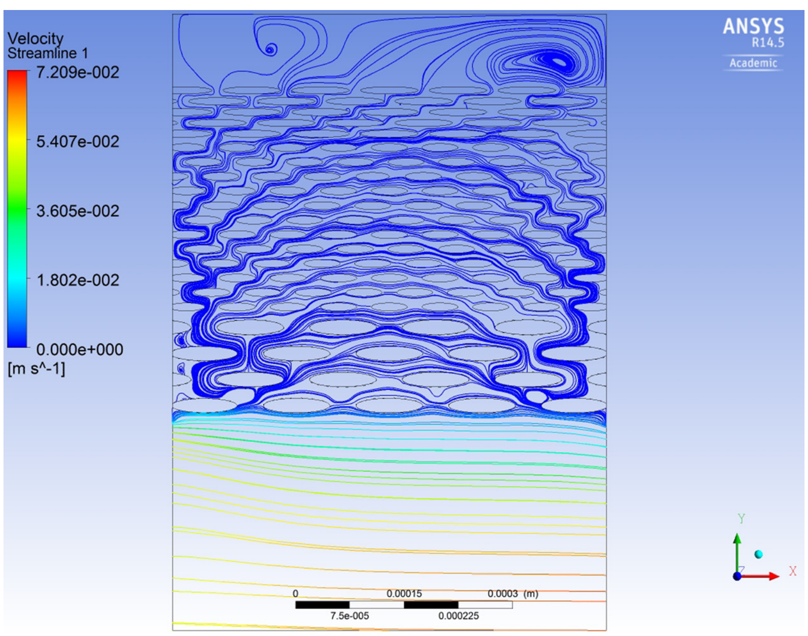

FIG. 9. Distribution of air flow velocity from the *A. pernyi* cocoon model at 1200 s in the oven with isothermal setting of 45 °C.

promote the survival chance of the silkworm pupa resides inside.[17]

V. CONCLUSION

The thermal insulation properties of silkworm cocoons in both hot and cold environments under windy conditions were investigated. The wild *A. pernyi* cocoon exhibits superior thermal buffer over the domestic *B. mori* cocoon. To study the heat transfer mechanism of this unique fibrous structure of the wild *A. pernyi* cocoon, a two dimensional CFD model of the *A. pernyi* cocoon was generated, the prediction of which agreed reasonably well with the experimental data.

Based on the findings from both experiments and modeling, it can be shown that the structure of the *A. pernyi* cocoon wall can promote the disorderness of the interior air; by prohibiting the air flowing from outside toward inside, the cocoon can reduce most of the heat flux by thermal convection. The existence of mineral crystals in the outer layers and the lower porosity and higher tortuosity in the middle and inner layers of the cocoon wall account for this unique function, which promotes the survival chance of the *A. pernyi* pupa under extreme weather conditions.

Nomenclature

c_v = effective volumetric heat capacity of the fibrous batting, J/(m^3 K)
c_{va} = effective volumetric heat capacity of the air, J/(m^3 K)
F = total thermal radiation, W
H = step function
p = pressure, Pa
p_{in} = static pressure on the inner surface of cocoon wall, Pa
p_{out} = static pressure on the outer surface of cocoon wall, Pa
p_s = static pressure, Pa
t = time, s
T = temperature, K
$T_{A.\,pernyi\text{–}in}$ = the temperature inside the *Antheraea pernyi* cocoon, K
$T_{B.\,mori\text{–}in}$ = the temperature inside the *Bombyx mori* cocoon, K
T_s = the surrounding temperature, K
$\bar{T}$ = extra-stress tensor
u = velocity, m/s
$\bar{u}$ = local velocity of the moving part, m/s
Γ = water accumulation rate, kg/(m^3 s)
ε = porosity of fibrous batting, dimensionless
κ = latent heat of sorption of fibers or condensation of water vapor, J/kg
λ = effective thermal conductivity of the fibrous batting, W/(m K)
ρa = the acceleration term
ρg = the volume force

ACKNOWLEDGMENT

The authors would like to acknowledge the funding support from the Australian Research Council (ARC) through a Project No. DP 120100139.

[1]E. J. W. Barber, *Prehistoric Textiles: The Development of Cloth in the Neolithic and Bronze Ages With Special Reference to the Aegean* (Princeton University, Princeton, NJ, 1991).
[2]Y.-H. S. Hong-Song Yu, G.-X. Yuan, Y.-G. Hu, H.-E. Xu, Z.-H. Xiang, and Z. Zhang, Mol. Biol. Evol. **28**, 1785 (2011).
[3]D. Normile, Science **325**, 1058 (2009).
[4]N. Hyde, Natl. Geogr. Mag. **165**, 2 (1984).
[5]K. P. Arunkumar, M. Metta, and J. Nagaraju, Mol. Phylogenet. Evol. **40**, 419 (2006).
[6]C. Acharya, S. K. Ghosh, and S. C. Kundu, Acta Biomater. **5**, 429 (2009).
[7]R. Rajkhowa, V. B. Gupta, and V. K. Kothari, J. Appl. Polym. Sci. **77**, 2418 (2000).
[8]S. Keten, Z. Xu, B. Ihle, and M. J. Buehler, Nature Mater. **9**, 359 (2010).
[9]X. Huang and W. Zhang, Adv. Mater. Res. **332–334**, 156 (2011).
[10]A. D. McNaught and A. Wilkinson, *Compendium of Chemical Terminology*. (Blackwell Science Oxford, Oxford, 1997).
[11]J. Pérez-Rigueiro, M. Elices, J. Llorca, and C. Viney, J. Appl. Polym. Sci. **84**, 1431 (2002).
[12]S. C. Kundu, B. C. Dash, R. Dash, and D. L. Kaplan, Prog. Polym. Sci. **33**, 998 (2008).
[13]A. G. B. Lima, S. R. Farias Neto, and W. P. Silva, *Heat and Mass Transfer in Porous Media*, edited by J. M. P. Q. Delgado (Springer, Berlin Heidelberg, 2012), Vol. 13, pp. 161–185.
[14]H.-P. Zhao, X.-Q. Feng, S.-W. Yu, W.-Z. Cui, and F.-Z. Zou, Polymer **46**, 9192 (2005).
[15]R. Rajkhowa, Int. J. Wild Silkmoths **5**, 287 (2000).
[16]G. Freddi, Y. Gotoh, T. Mori, I. Tsutsui, and M. Tsukada, J. Appl. Polym. Sci. **52**, 775 (1994).
[17]M. Roy, S. Meena, T. Kusurkar, S. Singh, N. Sethy, K. Bhargava, S. Sarkar, and M. Das, Biointerphases **7**, 1 (2012).
[18]F. Chen, D. Porter, and F. Vollrath, Mater. Sci. Eng., C **32**, 772 (2012).
[19]X. Chen and N. Chandra, Compos. Sci. Technol. **64**, 1477 (2004).
[20]L. Tsai and V. Prakash, Int. J. Solids Struct. **42**, 727 (2005).
[21]S. Zhuang, G. Ravichandran, and D. E. Grady, J. Mech. Phys. Solids **51**, 245 (2003).
[22]J. Zhang, J. Kaur, R. Rajkhowa, J. L. Li, X. Y. Liu, and X. G. Wang, Mater. Sci. Eng., C **33**, 3206 (2013).
[23]J. Zhang, R. Rajkhowa, J. L. Li, X. Y. Liu, and X. G. Wang, Mater. Des. **49**, 842 (2013).
[24]K. R. Avazov, Appl. Sol. Energy **45**, 133 (2009).
[25]J. O. Ukponmwan, Text. Prog. **24**, 1 (1993).
[26]J. Kaur, R. Rajkhowa, T. Afrin, T. Tsuzuki, and X. Wang, Biopolymers **101**, 237 (2014).
[27]ANSYS (LEAP Australia Pty. Ltd., Clayton North, Victoria, Australia, 2013).
[28]N. P. C. Horrocks, F. Vollrath, and C. Dicko, Comp. Biochem. Physiol., Part A **164**, 645 (2013).
[29]G. Liu, X. Huang, Y. Wang, Y.-Q. Zhang, and X. Wang, Soft Matter **8**, 9792 (2012).
[30]D. Rickenmann and A. Recking, Water Resour. Res. **47**, W07538 (2011).
[31]Y. Li and J. Fan, Numer. Heat Tranfer, Part A **51**, 635 (2007).
[32]ANSYS, *ANSYS CFX Handbook Version 14.5* (CFX Company, United Kingdom, 2013).
[33]F. Jintu, D. Ning, W. Huijun, and S. Weiwei, AIP Conf. Proc. **1233**, 1184 (2010).
[34]S.-M. Lee, Rev. Sci. Instrum. **80**, 024901 (2009).
[35]D. Wen and Y. Ding, Int. J. Heat Mass Tranfer **47**, 5181 (2004).
[36]M. J. Fuerstman, A. Lai, M. E. Thurlow, S. S. Shevkoplyas, H. A. Stone, and G. M. Whitesides, Lab Chip **7**, 1479 (2007).
[37]L. P. Lounibos, Anim. Behav. **23**, **Part** 4, 843 (1975).
[38]T. Kaise, M. Miura, H. Morikawa, and M. Iwasa, J. Insect Biotechnol. Sericol. **72**, 171 (2003).

[39]H.-P. Zhao, X.-Q. Feng, W.-Z. Cui, and F.-Z. Zou, Eng. Fract. Mech. **74**, 1953 (2007).
[40]J. Kou, Y. Liu, F. Wu, J. Fan, H. Lu, and Y. Xu, J. Appl. Phys. **106**, 054905 (2009).
[41]S. Maruyama, T. Kashiwa, H. Yugami, and M. Esashi, Appl. Phys. Lett. **79**, 1393 (2001).
[42]R. B. Barnes, Science **140**, 870 (1963).
[43]S. Mukhopadhyay, Int. J. Heat Mass Tranfer **52**, 3261 (2009).